0022-3565/03/3063-1129–1136$7.00
THE JOURNAL OF PHARMACOLOGY AND EXPERIMENTAL THERAPEUTICS
JPET 306:1129–1136, 2003

Vol. 306, No. 3
49429/1086503
Printed in U.S.A.

Comparative Effects of Methylmercury and Hg^{2+} on Human Neuronal N- and R-Type High-Voltage Activated Calcium Channels Transiently Expressed in Human Embryonic Kidney 293 Cells

RAVINDRA K. HAJELA,[1] SHUANG-QING PENG,[1] and WILLIAM D. ATCHISON

Department of Pharmacology and Toxicology, Institute of Environmental Toxicology and Neuroscience Program, Michigan State University, East Lansing, Michigan

Received January 22, 2003; accepted May 23, 2003

ABSTRACT

Expression cDNA clones of α_{1B-1} or α_{1E-3} subunits coding for human neuronal N- ($Ca_{v2.2}$) or R-subtype ($Ca_{v2.3}$) Ca^{2+} channels, respectively, was combined with $\alpha_{2-b}\delta$ and β_{3-a} Ca^{2+} channel subunits, and transfected into human embryonic kidney cells for transient expression to determine whether specific types of neuronal voltage-sensitive Ca^{2+} channels are affected differentially by methylmercury (MeHg) and Hg^{2+}. For both Ca^{2+} channel subtypes, MeHg (0.125–5.0 μM) or Hg^{2+} (0.1–5 μM) caused a time- and concentration-dependent reduction of current. MeHg caused an initial, rapid component and a subsequent more gradual component of inhibition. The rapid component of block was completed between 100 and 150 s after beginning treatment. At 0.125 to 1.25 μM, MeHg caused a more gradual decline in current. Apparent IC_{50} values were 1.3 and 1.1 μM for MeHg, and 2.2 and 0.7 μM for Hg^{2+} on N- and R-types, respectively. For N-type current, effects of Hg^{2+} were initially greater on the peak current than on the sustained current remaining at the end of a test pulse; subsequently, Hg^{2+} blocked both components of current. For R-type current, Hg^{2+} affected peak and sustained current approximately equally. Kinetics of inactivation also seemed to be affected by Hg^{2+} in cells expressing N-type but not R-type current. Washing with MeHg-free solution could not reverse effects of MeHg on either type of current. The effect of Hg^{2+} on N- but not R-type current was partially reversed by Hg^{2+}-free wash solution. Therefore, different types of Ca^{2+} channels have differential susceptibility to neurotoxic mercurials even when expressed in the same cell type.

Voltage-sensitive Ca^{2+} channels play crucial roles in a number of cellular functions, including neurotransmitter release, gene expression, growth cone elongation, and dendritic action potential generation (Catterall, 1998, 2000). Various Ca^{2+} channelopathies resulting in neuronal or neuromuscular disorders are caused by mutations in genes coding for Ca^{2+} channel subunits (for review, see Meir and Dolphin, 2002). At least six distinct subtypes of Ca^{2+} channels (L, N, T, P, Q, and R) have already been identified based on their differential biophysical, molecular biological, and pharmacological properties (Tsien et al., 1995). Neuronal Ca^{2+} channels contain four subunits: α_1, β, α_2, and δ. The α_1 subunit is the pore-forming, voltage-sensing, and ligand-binding component. cDNAs for at least seven distinct α subunits for high-voltage activated Ca^{2+} channels: α_{1A-1F}, α_{1S}, have been cloned. Four different β subunits and two different α_2 subunits regulate assembly and modulate the kinetic parameters of the channel. The presence of several isoforms and splice variants further complicates the functional expression characteristics and classification of high-voltage activated Ca^{2+} channels (Brust et al., 1993; DeWaard and Campbell, 1995; McEnery et al., 1998; Pan and Lipscombe, 2000). Cells typically coexpress several types of Ca^{2+} channels, often with similar subcellular localization, providing a highly regulated degree of control over Ca^{2+}-dependent cell functions, but confounding analyses of the properties of distinct Ca^{2+} channel subtypes in isolation. Because of their portal location within the plasma membrane, Ca^{2+} channels are potentially susceptible to the actions of a number of polyvalent heavy metal-type toxicants and serve as entry paths into the cell for heavy metals (Kiss and Osipenko, 1994; Atchison, 2003).

This study was supported by National Institutes of Health Grants R01ES03299 and R01ES05822 (to W.D.A.). A preliminary report of these findings was presented at the 2001 Annual Meeting of the Society of Toxicology in San Francisco, CA and published in *Toxicologist* **60:**185.

[1] R.K.H. and S.-Q.P. contributed equally to this study.

Article, publication date, and citation information can be found at http://jpet.aspetjournals.org.

DOI: 10.1124/jpet.103.049429.

ABBREVIATIONS: MeHg, methylmercury; I_{Ba}, Ba^{2+} current; HEK, human embryonic kidney; GFP, green fluorescent protein; $V_{1/2}$, voltage for half-maximal activation.

Because of the crucial roles that Ca^{2+} channels play in key cellular functions, toxicant effects on Ca^{2+} channels could have significant deleterious consequences for neuronal function.

Methylmercury (MeHg) and inorganic mercury (Hg^{2+}) are environmental neurotoxicants that differ chemically in ionic charge, ionic radii, and lipophilicity. Together, these factors can impact the manner in which these mercurials affect a given cellular function. Neurotoxic mercurials act on a number of cellular targets. In several neuronal systems, cellular effects of MeHg and Hg^{2+} are similar, yet distinct (Atchison et al., 1986; Hare and Atchison, 1992; Hewett and Atchison, 1992; Yuan and Atchison, 1994). The exact mechanisms by which these mercurials exert neurotoxicity are not known with certainty.

Disruption of function of voltage-sensitive Ca^{2+} channels is a prominent effect of acute exposure to low concentrations of both MeHg (Shafer and Atchison, 1991; Leonhardt et al., 1996; Sirois and Atchison, 1996, 2000; Shafer, 1998) and Hg^{2+} (Büsselberg et al., 1991; Weisenberg et al., 1995). MeHg blocks Ba^{2+} currents (I_{Ba}) carried through multiple subtypes of Ca^{2+} channels in primary cultures of cerebellar granule cells and in rat pheochromocytoma (PC12) cells (Shafer and Atchison, 1991; Sirois and Atchison, 2000). Hg^{2+} also alters function of several types of Ca^{2+} channels at low micromolar concentrations (Büsselberg et al., 1994; Leonhardt et al., 1996; Szucs et al., 1997). However, the actions of mercurials on Ca^{2+} channels may be more complex than mere block of function. In PC12 cells, very low concentrations of Hg^{2+} increase amplitude of current carried through voltage-sensitive Ca^{2+} channels (Rossi et al., 1993), whereas in cerebellar granule cells and NG108-15 cells, MeHg causes an increase in fura-2 fluorescence, which is dependent, at least in part, on extracellular Ca^{2+}, and which is delayed by nifedipine, ω-conotoxin GVIA, and Ni^{2+} (Hare and Atchison, 1995; Marty and Atchison, 1997). Moreover, treatment of rodents with Ca^{2+} channel blockers prevents the toxic effects of MeHg (Sakamoto et al., 1996), and Ca^{2+} channel blockers delay the onset of cerebellar granule cell death with MeHg (Marty and Atchison, 1997; Gasso et al., 2001). Finally, in cells lacking Ca^{2+} channels, the onset of intracellular action of MeHg is delayed, suggesting that Ca^{2+} channels provide a path of entry for MeHg into the cell (Edwards et al., 2002). Therefore, mercurials seem to interact with voltage-sensitive Ca^{2+} channels in a complex manner.

Because of the numerous and important roles that voltage-sensitive Ca^{2+} channels play in neuronal function, disruption of function of voltage-sensitive Ca^{2+} channels may be a significant contributory factor in mercurial-induced neurotoxicity. There are few published reports comparing the effects of different mercurials on function of voltage-sensitive Ca^{2+} channels (Hewett and Atchison, 1992; Szucs et al., 1997; Schirrmacher et al., 1998), and no comparative study on the effects of these two forms of mercury on defined types of voltage-sensitive Ca^{2+} channels exists.

The goal of the present study was to determine whether specific types of voltage-sensitive Ca^{2+} channels were affected differentially by MeHg or Hg^{2+}. We compared the effect of MeHg and Hg^{2+} on N-($Ca_{v2.2}$) and R-($Ca_{v2.3}$) types of voltage-sensitive Ca^{2+} channels expressed using cDNA copies of their genes transferred into human embryonic kidney cells (HEK293). These cells are nonexcitable and commonly used for heterologous expression of membrane proteins, including voltage-dependent Ca^{2+} channels (Williams et al., 1994; Perez-Garcia et al., 1995; Quefurth et al., 1998). Expression cDNA clones of $\alpha_{1B\text{-}1}$ or $\alpha_{1E\text{-}3}$ subunit were combined with $\alpha_{2\text{-}b}\delta$ and $\beta_{3\text{-}a}$ Ca^{2+} channel subunits of human neuronal origin for transient expression of N- and R-subtypes, respectively, of high-voltage activated Ca^{2+} channels. Jellyfish green fluorescent protein (GFP) was used as a cotransfection reporter.

Materials and Methods

Materials. HEK293 cells (ATCC CRL-1573) were purchased from American Type Culture Collection (Manassas, VA). All reagents were pure or ultrapure laboratory grade unless specifically noted otherwise. cAMP, EGTA, HEPES, ATP, ω-conotoxin GVIA, and tetrodotoxin were all obtained from Sigma-Aldrich (St. Louis, MO). Stock solutions (5 mM) of methylmercuric chloride (ICN Pharmaceuticals, Costa Mesa, CA) and (10 mM) $HgCl_2$ were prepared weekly in double-distilled water, from which test solutions were prepared daily in extracellular solution (see below). Plasmids containing expression cDNA clones of human neuronal Ca^{2+} channel subunits were generously provided by Dr. Kenneth A. Stauderman of SIBIA Neurosciences (San Diego, CA), now Merck Research Laboratories. $\alpha_{1E\text{-}3}$ (Williams et al., 1994) and $\beta_{3\text{-}a}$ subunit clones (Mark Williams, Merck Research Laboratories, personal communication) were isolated from hippocampus; $\alpha_{1B\text{-}1}$ was isolated from the IMR32 cell line (Williams et al., 1992b), and $\alpha_{2B}\delta$ was isolated from brainstem and basal ganglia (Williams et al., 1992a).

Cell Culture and Transfection. HEK293 cells were grown at 37°C in Eagle's minimal essential medium fortified with 1 mM sodium pyruvate, 0.1 mM nonessential amino acids, 2 mM L-glutamine, 1.5 g/l sodium bicarbonate, 10% (v/v) fetal bovine serum, and penicillin/streptomycin/amphotericin B (at a final concentration of 100 U/ml penicillin G, 100 μg/ml streptomycin sulfate, and 0.25 μg/ml amphotericin B; Invitrogen, Carlsbad, CA) in a 5% CO_2 environment. One day before gene transfer, cells were plated at a density of 5×10^5 on 35-mm culture dishes. Cells were transfected with a mixture of plasmids containing human neuronal $\alpha_{1B\text{-}1}$, or $\alpha_{1E\text{-}3}$ plus $\alpha_{2\text{-}b}\delta$ and $\beta_{3\text{-}a}$ Ca^{2+} channel subunits and a jellyfish GFP cDNA sequence using FuGENE 6 (Roche Diagnostics, Indianapolis, IN) following the manufacturer's instruction. Reactions contained a total of 3 μl of FuGENE 6 and 1 μg of plasmid DNA containing the three subunits in 1:1:1 M ratio, with GFP plasmid at 20% of the total DNA. Two days were allowed for transient expression of proteins at which time the cells were examined for GFP expression. Cells from dishes with a reasonable number of green fluorescent cells (usually 20%), were replated at a low density of sufficiently isolated individual cells to facilitate recording.

Ca^{2+} Channel Current Recording. Before recording, culture medium was removed, cells were rinsed twice with extracellular solution, and then replenished with 1 ml of extracellular recording solution. The extracellular solution contained 117 mM tetraethylammonium chloride, 20 mM $BaCl_2$, 1 mM $MgCl_2$, 25 mM D-glucose, 10 mM HEPES, and 0.001 mM tetrodotoxin; pH was adjusted to 7.2 at room temperature (~23–25°C) with tetraethylammonium hydroxide. The osmolarity of the solution was 310 mOsM. Patch-clamp pipettes with resistances between 6 and 8 MΩ were prepared from 1.5-mm i.d. glass capillaries (WPI, Sarasota, FL) using a two-stage microelectrode puller (PP-830; Narishige, Tokyo, Japan) and fire-polished using a Narishige MF-830 microforge. Intracellular (pipette) solution contained 140 mM CsCl, 10 mM EGTA, 10 mM HEPES, 2 mM ATP-Mg, and 1 mM cAMP; pH was adjusted to 7.2 with CsOH.

The tight seal whole cell configuration of the patch-clamp technique (Hamill et al., 1981) was used on fluorescent green cells to record I_{Ba} through transiently expressed Ca^{2+} channels. Whole cell currents were recorded using an Axopatch-1D amplifier (Axon In-

struments, Inc., Foster City, CA), sampled at 10 kHz and filtered at 2 kHz (−3 dB, four-pole Bessel filter; Axon Instruments, Inc.) and acquired on-line using the pClamp6 program (Axon Instruments, Inc.). Pipette and cell capacitance was compensated online in all experiments. Series resistance was also compensated in the range of 60 to 80%. Extracellular media were exchanged using a gravity-fed bath perfusion system (BPS-4; ALA Scientific Instruments, Westbury, NY); the flow rate was 5×10^{-3} ml/s. The distance of the flow pipette from the cell was maintained at approximately 150 μm. All experiments were carried out at room temperature (23–25°C).

To elicit I_{Ba}, the membrane was depolarized by a positive voltage step from the holding potential (−90 mV). Conventional voltage clamp step protocols were used to examine the amplitude of I_{Ba} over a range of membrane potentials and to examine the voltage dependence of activation of I_{Ba} and of steady-state inactivation of I_{Ba}. In experiments designed to examine the effects of Ni^{2+}, Cd^{2+}, MeHg, Hg^{2+}, or ω-conotoxin GVIA on I_{Ba}, the membrane was repeatedly (0.1 Hz) depolarized (from −90 mV) by a voltage step to 0 mV (R-type) or to 20 mV (N-type). Each depolarization was preceded by a hyperpolarizing voltage step (one-quarter the amplitude of the depolarizing step) to permit measurement of leakage current. After establishing that the current elicited by each depolarizing step was eventually constant, the test compound (modulator) was applied to the cell as mentioned above. Unless noted otherwise, in all experiments I_{Ba} amplitude was measured after subtraction of leak current from the whole current elicited by the activating depolarization.

Statistical Analysis. For each experiment recordings were made from a minimum of five cells, and these cells were derived from at least three independent transfections. Values are expressed as the mean ± S.E.M. The number of replicates is indicated for each experiment in the figure legend. Curve fitting of data points on graphs was performed using Origin software (OriginLab Corp., Northampton, MA).

Results

Characteristics of Recombinant Transiently Expressed α_{1B} and α_{1E} Subunit-Mediated Ca^{2+} Channel Currents in HEK293 Cells. Basic biophysical and pharmacological qualities of Ca^{2+} channels containing α_{1B} ($Ca_{v\,2.2}$) or α_{1E} ($Ca_{v\,2.3}$) subunit in combination with $\alpha_{2\text{-}b}\delta$ and $\beta_{3\text{-}a}$ subunits and expressed transiently in HEK293 cells were similar to those of N-or R-type Ca^{2+} channels, respectively, as expressed in their native environment. A constant set of $\alpha_{2\text{-}b}\delta$ and $\beta_{3\text{-}a}$ subunits was used in all experiments so that we could focus on the comparative actions of the two mercurials on the principal phenotype-defining subunit of voltage-sensitive Ca^{2+} channels, the α_1 subunit. Representative tracings of I_{Ba} elicited from these cells along with their current-voltage relationships and voltage dependence of steady-state inactivation and activation are shown in Fig. 1, A to C (for α_{1B}) and Fig. 2, A to C (for α_{1E}), respectively. For α_{1B}-containing channels, current seemed to activate at approximately −20 mV, reached peak amplitude at about +20 mV and reversed at +60 mV. For channels containing α_{1E} subunit, current activated at −40 mV, reached a peak amplitude at 0 mV and reversed at approximately +60 mV. The voltage for half-maximal activation ($V_{1/2}$) was 0 mV in α_{1B}-containing channels (Fig. 1C) and −14.8 mV in α_{1E}-containing channels (Fig. 2C), respectively. The isochronal inactivation (h) was determined using an 8-s inactivating prepulse. The inactivation curves are shown (Figs. 1C and 2C) with slope parameter (k) of 12.0 mV and $V_{1/2}$ of −64.6 mV for α_{1B}-containing channels,

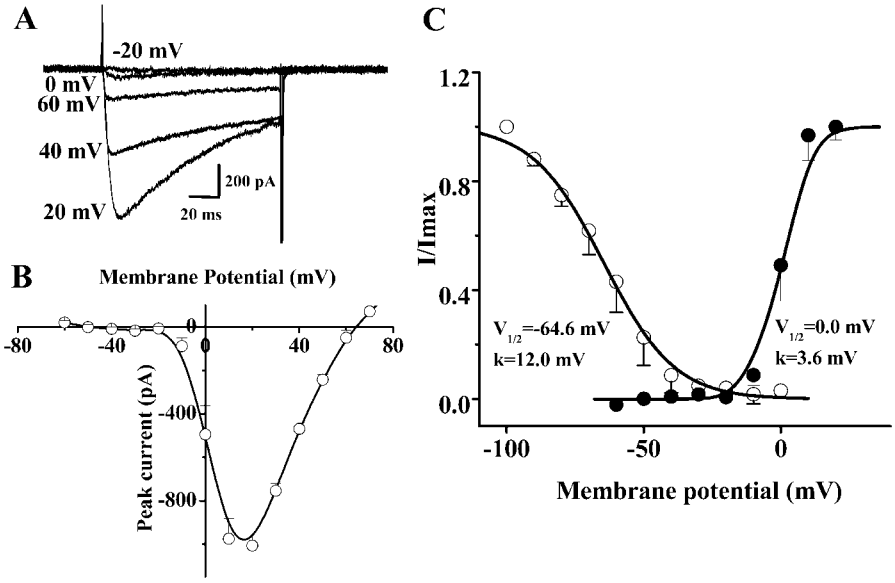

Fig. 1. Biophysical characteristics of whole cell Ba^{2+} current mediated by recombinant N-type Ca^{2+} channels expressed in HEK293 cells. A, representative family of current traces (filtered at 2 kHz but not leak subtracted) elicited by voltage steps from a holding potential of −90 mV to test potentials ranging from −20 to +60 mV. Ba^{2+} (20 mM) was used as the charge carrier. B, current-voltage relationship for the Ba^{2+} current was derived from the type of experiment illustrated in A. The peak current elicited during a voltage step is plotted as a function of the test potential. C, voltage dependence of activation (●) and of steady-state inactivation (○) is depicted. To examine voltage dependence of activation, peak current elicited during a depolarizing voltage step from the holding potential to each test potential was normalized to the maximum current elicited and normalized current was plotted as a function of test potential. Data points were fitted by the curve using a Boltzmann function: $I/I_{max} = [1 + \exp\{(V - V_{1/2})/k\}]^{-1}$, with $V_{1/2} = -64.6$ mV and $k = 12.0$ mV. To examine the voltage dependence of steady-state inactivation, a conditioning voltage step (8 s, to potentials between −100 and 0 mV, in 10-mV increments) was applied to allow inactivation of the channel to achieve steady state, and the membrane was then stepped to +20 mV. Current elicited at +20 mV after each conditioning step was measured and normalized to amplitude elicited (at +20 mV) after a conditioning step to −100 mV. Normalized current was plotted as a function of conditioning (step) potential. Data points were fitted by the curve using a Boltzmann function: $I/I_{max} = [1 + \exp\{-(V - V_{1/2})/k\}]^{-1}$, with $V_{1/2} = 0.0$ mV and $k = 3.6$ mV. Ba^{2+} current amplitude was measured after subtraction of leak current from the whole current elicited by the activating depolarization. In B and C, values shown are the mean ± S.E.M. of 10 cells.

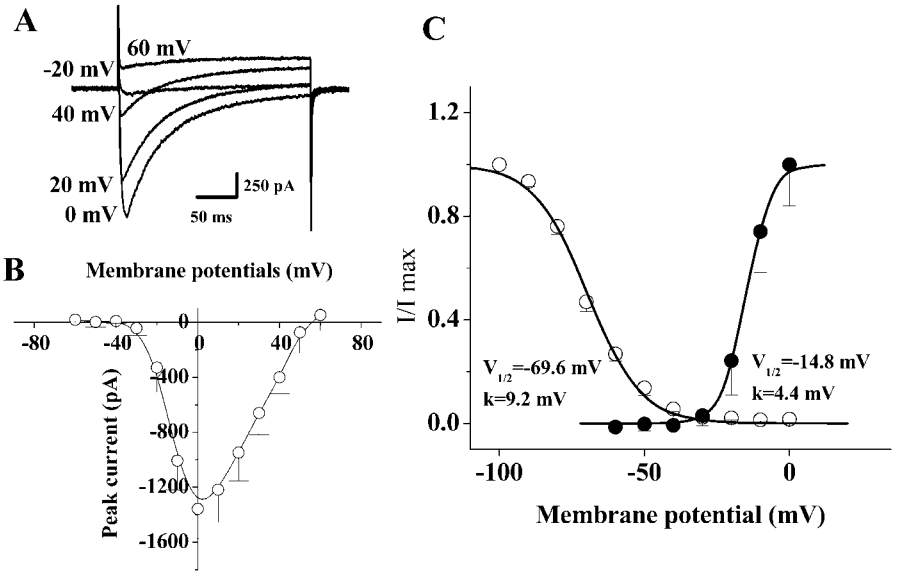

Fig. 2. Biophysical characteristics of whole cell Ba^{2+} current mediated by recombinant R-type Ca^{2+} channels expressed in HEK293 cells. A, representative family of current traces (filtered at 2 kHz but not leak subtracted) elicited by voltage steps from a holding potential of −90 mV to test potentials ranging from −20 to +60 mV. Ba^{2+} (20 mM) was used as the charge carrier. B, current-voltage relationship for the I_{Ba} was derived from the type of experiment illustrated in A. The peak current elicited during a voltage step is plotted as a function of the test potential. C, voltage dependence of activation (●) and of steady-state inactivation (○). To examine voltage dependence of activation, peak current elicited during a depolarizing voltage step from the holding potential to each test potential was normalized to the maximum current elicited and normalized current was plotted as a function of test potential. Data points were fitted by the curve using a Boltzmann function: $I/I_{max} = [1 + \exp\{(V - V_{1/2})/k\}]^{-1}$, with $V_{1/2} = -69.6$ mV and $k = 9.2$ mV. To examine the voltage dependence of steady-state inactivation, a conditioning voltage step (8 s, to potentials between −100 and 0 mV, in 10-mV increments) was applied to allow inactivation of the Ba^{2+} current to come to steady state, and the membrane potential was then stepped to +20 mV. Current elicited at +20 mV after each conditioning step was measured and normalized to amplitude elicited (at +20 mV) after a conditioning step to −100 mV. Normalized current was plotted as a function of conditioning (step) potential. Data points were fitted by the curve using a Boltzmann function: $I/I_{max} = [1 + \exp\{-(V - V_{1/2})/k\}]^{-1}$, with $V_{1/2} = -14.8$ mV and $k = 4.4$ mV. Ba^{2+} current amplitude was measured after subtraction of leak current from the whole current elicited by the activating depolarization. Values shown in B and C are the mean ± S.E.M. of seven cells.

and k of 9.2 mV and $V_{1/2}$ of −69.6 mV for α_{1E}-containing channels, respectively.

Figure 3 demonstrates that I_{Ba} expressed in cells transfected with α_{1B} subunit was sensitive to inhibition by ω-conotoxin GVIA. At 1 or 10 μM, ω-conotoxin GVIA caused a rapid reduction of current amplitude; the rate with which block occurred was concentration-dependent. However, ultimately, both concentrations blocked virtually all current. The effect of ω-conotoxin block was not reversed by washing the cell with toxin-free solution. Thus, the I_{Ba} recorded from HEK293 cells expressing human neuronal α_{1B} subunits combined with a fixed complement of $\alpha_2\delta\beta_3$ subunits has biophysical and pharmacological properties consistent with those mediated by N-type Ca^{2+} channels. We tested α_{1E} subunit-expressing HEK293 cells with known specific antagonists (nimodipine and ω-agatoxin IVA) for the L- or P/Q-type channels and found the I_{Ba} to be resistant to block by both of these agents (data not shown), consistent with the characteristics of R-type current. Therefore, we used varying concentrations of Cd^{2+} and Ni^{2+} (both of which are known to block current carried through all known subtypes of voltage-sensitive Ca^{2+} channels) on the α_{1E} subunit-containing cells (Fig. 4, A and B). The block of I_{Ba} from these cells by both divalent cations was concentration-dependent. A stepwise reduction of current was seen after addition of successively higher concentrations of Cd^{2+} or Ni^{2+}; this effect seemed to plateau until the next higher concentration of metal was added. The reduction of amplitude of I_{Ba} was complete at 100 μM Cd^{2+} or 1 mM Ni^{2+}. These two observations together indicate that the pharmacological characteristics of α_{1E} subunit-mediated I_{Ba} from these cells is consistent with that of the R-type. An interesting observation at the lowest concentrations of Cd^{2+} (0.1 μM; Fig. 4A) and Ni^{2+} (1 μM; Fig. 4B) was an apparent slight increase rather than reduction in amplitude of I_{Ba}. This effect was more prominent with Cd^{2+}.

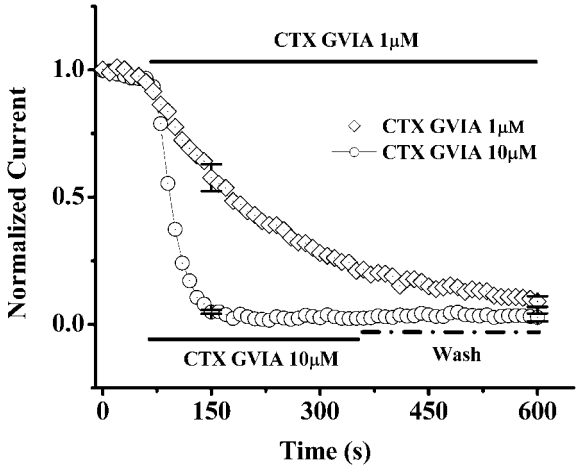

Fig. 3. Effect of 1.0 and 10.0 μM ω-conotoxin GVIA (ω-CgTx GVIA) on peak Ba^{2+} current (20 mM Ba^{2+}) amplitude in HEK293 cells expressing human neuronal α_{1B} subunit containing N-type Ca^{2+} channels. At 10.0 μM, ω-CgTx GVIA caused an almost complete and irreversible block of Ba^{2+} current, because current could not be restored by washing cells with toxin-free extracellular solution. Cells were depolarized from −90 to +20 mV at a stimulation frequency of 0.1 Hz. Current responses were filtered at 2 kHz and leak current was subtracted. Values shown are the mean of five to six cells. To simplify the figure only representative S.E.M. values are shown.

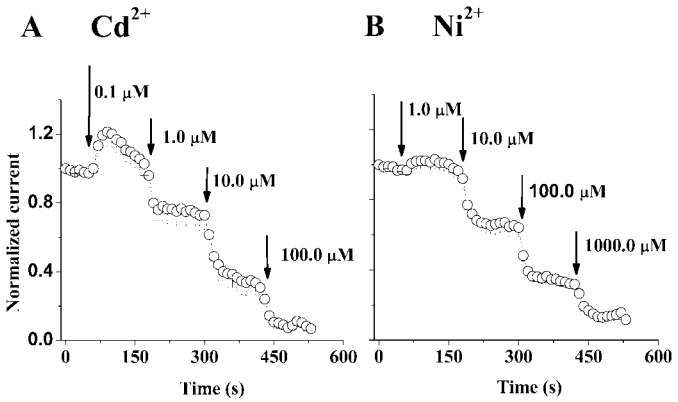

Fig. 4. Effect of different concentrations of Cd^{2+} (A) and Ni^{2+} (B) on peak Ba^{2+} current (20 mM Ba^{2+}) amplitude from HEK293 cells expressing human neuronal α_{1E} subunit mediated R-type Ca^{2+} channels. Notice the stepwise reduction of current amplitude with each higher concentration of Cd^{2+} or Ni^{2+} addition that seems to plateau until the next higher concentration is added. The block of Ba^{2+} current becomes complete at 100 μM Cd^{2+} and 1 mM Ni^{2+}. Cells were depolarized from −90 to 0 mV at a stimulation frequency of 0.1 Hz. Current responses were filtered at 2 kHz and leak current was subtracted. Values shown are the mean ± S.E.M. of six to seven cells.

Perhaps this effect is due to these cations actually entering the Ca^{2+} channels based on their relatively similar ionic radii and electrical charges. These same cations become inhibitory at higher concentrations.

Time- and Concentration Dependence of MeHg Effect on I_{Ba}. As shown in Figs. 5A and 6A for representative traces, and in composite data from a number of preparations in Figs. 5B and 6B, MeHg caused a rapid, concentration- and time-dependent reduction in current from both α_{1B} and α_{1E} subunit-containing channels. As shown in Fig. 5A for cells expressing α_{1B}-type current, the effect of 5 μM MeHg was initially greater on the peak current than on the sustained current remaining at the end of a test pulse. However, with additional time, MeHg blocked both components of current apparently equally. For cells expressing α_{1E} subunit, the degree of block of current by 5 μM MeHg seemed to be approximately the same for both peak and sustained current (Fig. 6A). The effect of different concentrations of MeHg on

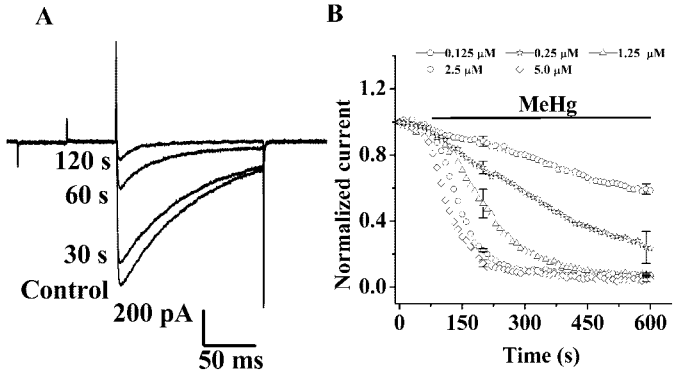

Fig. 5. Effect of MeHg on peak Ba^{2+} current (20 mM Ba^{2+}) amplitude from HEK293 cells expressing human neuronal α_{1B} subunit-containing N-type Ca^{2+} channels. A, representative current traces showing the effect of 5.0 μM MeHg on peak current at different times of exposure. B, time course of block of peak current by different concentrations of MeHg. Cells were depolarized from −90 to +20 mV at a stimulation frequency of 0.1 Hz. Current responses were filtered at 2 kHz and leak current was subtracted. Values shown are the mean of five to seven cells. To simplify the figure only representative S.E.M. values are shown.

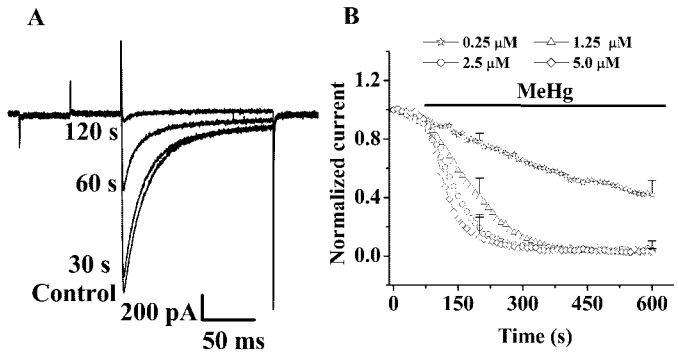

Fig. 6. Effect of MeHg on peak Ba^{2+} current (20 mM Ba^{2+}) amplitude from HEK293 cells expressing human neuronal α_{1E} subunit-containing R-type Ca^{2+} channels. A, representative current traces showing the effect of 5.0 μM MeHg on peak current amplitude at different times of exposure. B, time course of block of peak Ba^{2+} current by different concentrations of MeHg. Cells were depolarized from −90 to 0 mV at a stimulation frequency of 0.1 Hz. Current responses were filtered at 2 kHz and leak current was subtracted. Values shown are the mean of five to seven cells. To simplify the figure only representative S.E.M. values are shown.

whole cell I_{Ba} with either subunit is shown as a time course in Figs. 5B and 6B and was determined after at least 5-min stabilization of the control current. Addition of MeHg concentrations between 0.125 (or 0.25 for α_{1E} subunit) and 5.0 μM to the extracellular solution resulted in a concentration-dependent block in the rate and magnitude of I_{Ba} after leak subtraction. For both kinds of channels, the block of peak current by MeHg was again concentration- and time-dependent. MeHg concentrations in excess of 1 μM caused complete block of current within 2 to 6 min. Submicromolar concentrations also caused measurable inhibition (Figs. 5B and 6B). The rate at which inhibition occurred at micromolar concentrations seemed to consist of two distinct components: one which was initially more rapid, and the other, which was more gradual (Figs. 5B and 6B). Depending upon the concentration of MeHg used, the rapid component was completed between 100 and 150 s after beginning treatment. Lower concentrations of MeHg (0.125–1.25 μM) caused a more gradual decline in current amplitude. Inhibition of current at 1.25 μM MeHg seemed ultimately to reach the same plateau as at higher concentrations. At 0.125 μM in α_{1B}- and 0.25 μM in α_{1E}-containing channels, inhibition never reached the same level as at higher concentrations over the 10-min recording period. Because lower concentrations of MeHg caused a slow, progressive block of current that didn't reach a plateau, we could only estimate an apparent IC_{50} value for MeHg. This was done by comparing the percentage of block at each concentration at a set time point. At 200 s, MeHg blocked ~50% of both types of current at 1.3 (N-type) and 1.1 μM (R-type).

Concentration Dependence of Hg^{2+} Effect on I_{Ba}. Figures 7 and 8 show the effects of Hg^{2+} on I_{Ba} from HEK293 cells expressing α_{1B} and α_{1E} subunit-containing Ca^{2+} channels, respectively. Figures 7A and 8A depict representative current traces showing effects of different concentrations of Hg^{2+} on current after 2-min exposure. Hg^{2+} caused a rapid, concentration-dependent reduction in current from both α_{1B} and α_{1E} subunit-expressing channels. As shown in Fig. 7A for cells expressing α_{1B}-type current, the effect of 0.5, 1, and 5.0 μM Hg^{2+} was initially greater on the peak current than on the sustained current remaining at the end of a test pulse.

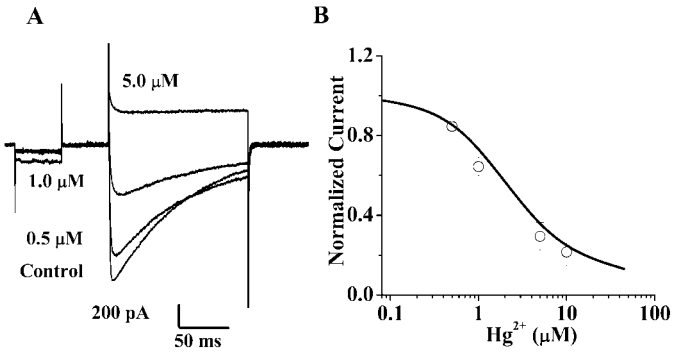

Fig. 7. Effect of Hg^{2+} on peak Ba^{2+} current (20 mM Ba^{2+}) amplitude from HEK293 cells expressing human neuronal α_{1B} subunit-containing N-type Ca^{2+} channels. A, representative current traces showing effect of different concentrations of Hg^{2+} on peak current amplitude after 2-min exposure. B, peak currents recorded after a 2-min exposure to different concentrations of Hg^{2+} were fitted using the equation $I_{[Hg2+]}/I_{Control} = [1 + ([Hg^{2+}]_e/IC_{50})^n]^{-1}$ with IC_{50} = 2.2 μM. Only a single concentration of Hg^{2+} was applied per cell. Cells were depolarized from −90 to +20 mV at a stimulation frequency of 0.1 Hz. Current responses were filtered at 2 kHz and leak current was subtracted. Values shown are the mean ± S.E.M. of six cells.

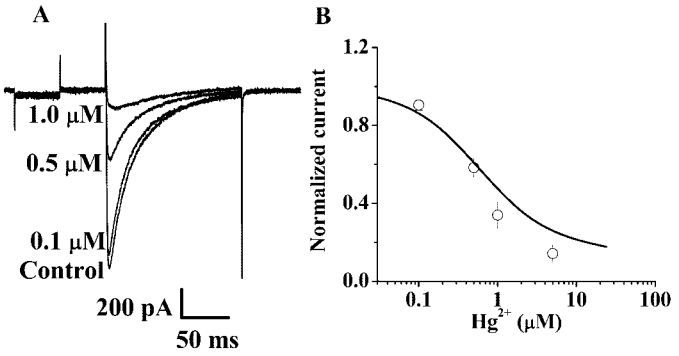

Fig. 8. Effect of Hg^{2+} on peak Ba^{2+} (20 mM) current amplitude from HEK293 cells expressing human neuronal α_{1E} subunit-containing R-type Ca^{2+} channels. A, representative current traces showing effect of different concentrations of Hg^{2+} on peak current after 2-min exposure. B, peak currents recorded after a 2-min exposure to different concentrations of Hg^{2+} were fitted using the equation $I_{[Hg2+]}/I_{Control} = [1 + ([Hg^{2+}]_e/IC_{50})^n]^{-1}$ with IC_{50} = 0.7 μM. Only a single concentration of Hg^{2+} was applied per cell. Cells were depolarized from −90 to 0 mV at a stimulation frequency of 0.1 Hz. Current responses were filtered at 2 kHz and leak current was subtracted. Values shown are the mean ± S.E.M. of five cells.

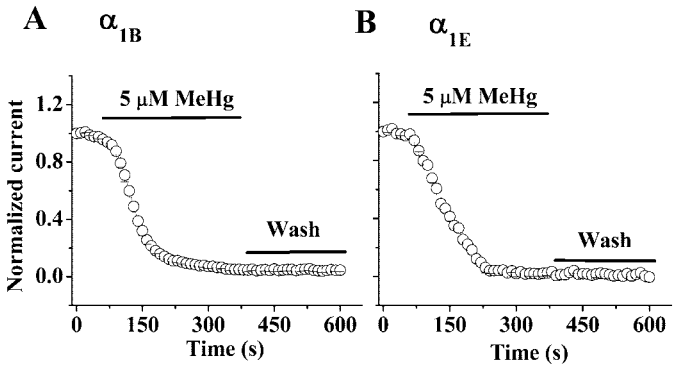

Fig. 9. Irreversible block by MeHg of Ba^{2+} current (20 mM Ba^{2+}) in HEK293 cells expressing α_{1B} or α_{1E} subunit-containing human neuronal Ca^{2+} channels. A 5-min treatment with 5 μM MeHg was followed by wash with MeHg-free solution. Cells were depolarized at a stimulation frequency of 0.1 Hz from −90 to +20 mV for cells with channels containing α_{1B} and −90 to 0 mV for those containing α_{1E}. Current responses were filtered at 2 kHz and leak current was subtracted. Values shown are the mean ± S.E.M. of five to seven cells.

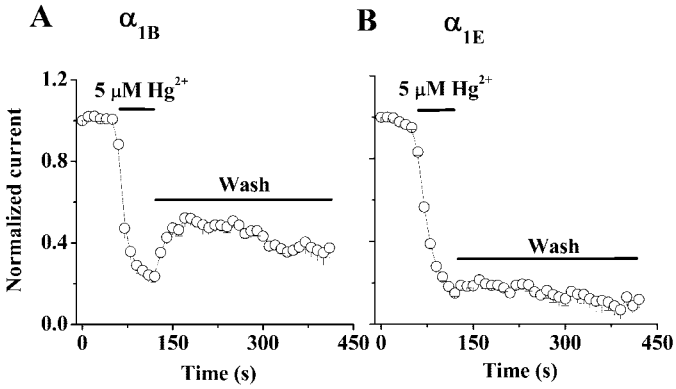

Fig. 10. Effects of wash with Hg^{2+}-free solution on block of I_{Ba}. A, block by 5 μM Hg^{2+} of peak Ba^{2+} current (20 mM Ba^{2+}) in HEK293 cells expressing α_{1B} subunit-containing human neuronal Ca^{2+} channels after a 1-min exposure is partially reversed by wash with Hg^{2+}-free solution. B, block by 5 μM Hg^{2+} of peak Ba^{2+} current in HEK293 cells expressing α_{1E} subunit-containing human neuronal Ca^{2+} channels after a 1-min exposure was not reversed by wash with Hg^{2+}-free solution. Cells were depolarized from −90 to +20 mV for α_{1B} and −90 to 0mV for α_{1E}. Current responses were filtered at 2 kHz and leak current was subtracted. Values shown are the mean ± S.E.M. of five to seven cells.

However, with additional time, Hg^{2+} blocked both components of current. For cells expressing α_{1E} subunit, the degree of block by 0.1, 0.5, and 1 μM Hg^{2+} seemed to be approximately the same for both peak and sustained current (Fig. 8A). Furthermore, the inactivation kinetics seems to be affected by Hg^{2+} in cells expressing α_{1B}-type current. Figures 7B and 8B depict the degree of reduction of normalized I_{Ba} as a function of concentration of Hg^{2+}. The IC_{50} values for Hg^{2+}-induced block of α_{1B} and α_{1E}-type current were 2.2 and 0.7 μM, respectively.

Effect of Wash with MeHg- or Hg^{2+}-Free Solution on I_{Ba}. As shown in Fig. 9, the block by MeHg of either type of current could not be reversed by washing with MeHg-free solution. However, the Hg^{2+} induced reduction of I_{Ba} through α_{1B}-mediated N-type channels was partially reversible (Fig. 10A), but the I_{Ba} reduction from α_{1E}-mediated R-type channels was not reversed by washing with Hg^{2+}-free solution (Fig. 10B).

Discussion

Previous studies have shown that MeHg (Shafer and Atchison, 1991; Marty and Atchison, 1997; Shafer, 1998; Sirois and Atchison, 2000) and Hg^{2+} (Büsselberg et al., 1994; Leonhardt et al., 1996; Szucs et al., 1997) affect the function of native Ca^{2+} channels in multiple types of cells. However, in most of these studies, the cells examined express more than one subtype of Ca^{2+} channels, and attempts to compare the actions of these metals on known subtypes of Ca^{2+} channel were incomplete and/or indirect. Until recently (Peng et al., 2002), there have been no studies of effects of mercurials on distinct subtypes of Ca^{2+} channel in isolation. The present study using transient expression of human neuronal Ca^{2+} channels is the first to characterize and compare the effects of the organomercurial MeHg and inorganic Hg^{2+} on current mediated by single, identified phenotypes (N- and R-type) of Ca^{2+} channel in isolation. Because the two types of expressed Ca^{2+} channel contained the same $\alpha_2\delta$ and β subunits, differential effects of the mercurials on expressed N- and R-type

channel current must be due largely to the mercurial interactions with, or action on, the α_1 pore-forming subunit of the channel. Our results support and extend several aspects of previous studies of mercurials on native N-type and R-type Ca^{2+} channels. Our results demonstrate that, first, MeHg is an irreversible and essentially equipotent inhibitor of current recorded from HEK293 cells expressing human neuronal α_{1B} (N-type) or α_{1E} (R-type) subunit containing Ca^{2+} channels. Second, although Hg^{2+} inhibits current mediated by the same channels, it has a more potent effect on recombinant R-type channels than N-type channels. Third, the effect of Hg^{2+} is partially reversible for recombinant N-type channels but is evidently irreversible for R-type channels.

Our recordings show that the voltage- and time-dependent characteristics of the current mediated by channels containing the α_{1B} subunit and those containing the α_{1E} subunit expressed in transfected cells resemble those of native N- and R-type Ca^{2+} channels, respectively, in neurons (Randall and Tsien, 1995). The different biophysical characteristics of native N-type channel current and current mediated by recombinant channels containing the α_{1B} subunit and of native R-type channel current and current mediated by recombinant channels containing the α_{1E} subunit may simply reflect differences of the $\alpha_2\delta$ and β subunits expressed in recombinant and native channels. Alternatively, these differences may be due to differences of the human α_1 subunits expressed in cells studied here and the α_1 subunits of the native channels of nonhuman derived neurons such as those studied by Randall and Tsien (1995). Furthermore, we have demonstrated that recombinant channels containing the α_{1B} subunit are sensitive to ω-conotoxin GVIA as are native N-type Ca^{2+} channels, whereas those channels expressing the α_{1E} subunit were highly sensitive to block by Cd^{2+} and to a lesser extent Ni^{2+} as is the case for native R-type channels.

The data presented here show that recombinant expressed N-type channels were more sensitive to the effects of MeHg than were presumptive N-type native channels in PC12 cells (Shafer and Atchison, 1991; Shafer, 1998) and dorsal root ganglion cells (Leonhardt et al., 1996) but were equally sensitive compared with presumptive N-type channels of rat cerebellar granule cells (Sirois and Atchison, 2000). Such differential sensitivity of native and recombinant expressed channels has also been reported for other toxins, including calcicludine effects on L-type channels (Stotz et al., 2000), ω-agatoxin IVA effects on P/Q-type channels (Bourinet et al., 1999), and peptide spider toxin DW13.3 effects on N-type channels (Sutton et al., 1998). These differential effects of mercurials and other toxins on recombinant and native channels may reflect differences between human and nonhuman α_1 subunits (present in studies of recombinant channels and native channels, respectively), or between the accessory ($\alpha_2\delta$ and β) subunits of various native channels and recombinant channels.

The present study of mercurials on recombinant Ca^{2+} channels also confirms previous observations concerning several aspects of the effect of MeHg on native channels. First, as has been observed for native channels in cerebellar granule cells (Sirois and Atchison, 2000) and PC12 cells (Shafer and Atchison, 1991), the effect of MeHg on recombinant α_{1B}-(N-type) and α_{1E} (R-type)-containing channels was not voltage-dependent. Second, the reduction of current during exposure to MeHg was irreversible regardless of whether the current was mediated by channels containing the α_{1B} (N-type) or α_{1E} (R-type) subunit or by various types of native Ca^{2+} channel. Third, it is also noteworthy that the effect of MeHg proceeds to complete reduction of the current mediated by channels containing the α_{1B} (N-type) or α_{1E} (R-type) subunit and by at least some native channels (given a sufficient duration of exposure to MeHg), although this effect was not observed for MeHg effects on recombinant α_{1C} (L-type) subunit-containing channels (Peng et al., 2002). Fourth, the effect of Hg^{2+} on native channels, which has variously been reported to be reversible or irreversible (Leonhardt et al., 1996), was found in the present study to be partially reversible for channels containing the α_{1B} (N-type) subunit, but evidently irreversible, for channels containing the α_{1E} (R-type) subunit. Although mechanisms associated with reversibility were not examined, this observation may help to explain the variability of reversal seen in studies with Hg^{2+} of native channels, inasmuch as, depending upon the complement of channel phenotype in the preparation being studied, the actions of Hg^{2+} may be more or less reversible. In the case of the irreversible effect of MeHg or Hg^{2+}, it is possible that the mercurial binds covalently to the channel (so that the mercurial cannot be removed) or interacts in some way with the channel that is irreversible (even after removal of the mercurial). Again, differences concerning the reversibility of a mercurial effect on native channels and on recombinant channels may reflect differences between the α_1 subunit or the accessory units of the native and recombinant Ca^{2+} channels. Regardless of the reversibility of the interaction of Hg^{2+} or MeHg with the channel, the specific site of interaction between mercurial and channel is unclear. Hg^{2+} or MeHg could act directly in the channel pore, have nonspecific or specific interactions with negatively charged groups on the cell surface, or act at a regulatory or allosteric binding site on the intra- or extracellular surface of the channel. However, it should be noted that Shafer (1998) reported that intracellular application of MeHg did not affect Ca^{2+} channel current in PC12 cells. Another difference between the effects of Hg^{2+} on recombinant and native channels is that Hg^{2+} seems to increase Ca^{2+} current through native channels at low concentration (Manalis and Cooper, 1975; Rossi et al., 1993); this phenomenon was not observed in our study of recombinant channels.

In summary, both MeHg and Hg^{2+} perturb the function of heterologously expressed, recombinant human neuronal N-type and R-type Ca^{2+} channels at low micromolar concentrations, well within the range of concentrations known to cause disruption of function of corresponding native channels as well as toxicity from these agents in vivo. MeHg was an equipotent inhibitor of human neuronal N-type and R-type Ca^{2+} channels expressed in HEK293 cells. However, there seem to be subtle differences on the effects of Hg^{2+}, which vary somewhat depending on the type of α_1 subunit.

Acknowledgments

We acknowledge the generous contribution of the Ca^{2+} channel cDNA clones by SIBIA Neurosciences (now Merck Research Laboratories, San Diego, CA). Thanks are also due to Dr. Peter J. R. Cobbett (Department of Pharmacology and Toxicology, Michigan State University) for critical reading of the manuscript and valuable discussion. The excellent secretarial assistance of Mallory Koglin and Kelly O'Brien is especially appreciated.

References

Atchison WD (2003) Effects of toxic environmental contaminants on voltage-gated calcium channel function: from past to present. *J Bioenerg Biomembr*, in press.

Atchison WD, Joshi U, and Thornburg JE (1986) Irreversible suppression of calcium entry into nerve terminals by methylmercury. *J Pharmacol Exp Ther* **238:**618–624.

Bourinet E, Soong TW, Sutton K, Slaymaker S, Mathews E, Monteil A, Zamponi GW, Nargeot J, and Snutch TP (1999) Splicing of α_{1A} subunit gene generates phenotypic variants of P- and Q-type calcium channels. *Nat Neurosci* **2:**407–414.

Brust PF, Simerson S, McCue AF, Deal CR, Schoonmarker S, Williams ME, Velicelebi G, Johnson EC, Harpold MM, and Ellis SB (1993) Human neuronal voltage-dependent calcium channels: studies on subunit structure and role in channel assembly. *Neuropharmacology* **32:**1089–1102.

Büsselberg D, Pekel M, Michael D, and Platt B (1994) Mercury and zinc: two divalent cations with different actions on voltage-activated calcium channel currents. *Cell Mol Neurobiol* **14:**675–687.

Büsselberg D, Vans M, Rahmann H, and Carpenter D (1991) Effects of inorganic and triethyl lead and inorganic mercury on the voltage activated calcium channels of *Aplysia* neurons. *Neurotoxicology* **12:**733–744.

Catterall WA (1998) Structure and function of neuronal Ca^{2+} channels and their role in neurotransmitter release. *Cell Calcium* **24:**307–323.

Catterall WA (2000) Structure and regulation of voltage-gated Ca^{2+} channels. *Annu Rev Cell Dev Biol* **16:**521–555.

DeWaard M and Campbell KP (1995) Subunit regulation of the neuronal α_{1A} Ca^{2+} channel expressed in *Xenopus* oocytes. *J Physiol (Lond)* **485:**619–634.

Edwards JR, Cobbett P, and Atchison WD (2002) Comparative disruption of intracellular calcium regulation by methylmercury in PC12 and PC18 cells. *Soc Neurosci Abstr*, *Abstracts Viewer/Itinerary Planner* 833.5.

Gasso S, Cristofol RM, Selema G, Rosa R, Rodriguez-Farre E, and Sanfeliu C (2001) Antioxidant compounds and Ca^{2+} pathway blockers differentially protect against methylmercury and mercuric chloride neurotoxicity. *J Neurosci Res* **66:**135–145.

Hamill OP, Marty A, Neher E, Sakmann B, and Sigworth FJ (1981) Improved patch-clamp techniques for high-resolution current recording from cells and cell-free membrane patches. *Pfluegers Arch* **391:**85–100.

Hare MF and Atchison WD (1992) Comparative action of methylmercury and divalent inorganic mercury on nerve terminal and intraterminal mitochondrial membrane potentials. *J Pharmacol Exp Ther* **261:**166–172.

Hare MF and Atchison WD (1995) Nifedipine and tetrodotoxin delay the onset of methylmercury induced increase in $[Ca^{2+}]_i$ in NG108-15 cells. *Toxicol Appl Pharmacol* **135:**299–307.

Hewett SJ and Atchison WD (1992) Effects of charge and lipophilicity on mercurial-induced reduction of $^{45}Ca^{2+}$ uptake in isolated nerve terminals of the rat. *Toxicol Appl Pharmacol* **113:**267–273.

Kiss T and Osipenko ON (1994) Toxic effects of heavy metals on ionic channels. *Pharmacol Rev* **46:**245–267.

Leonhardt R, Pekel M, Platt B, Haas HL, and Büsselberg D (1996) Voltage-activated calcium channel currents of rat DRG neurons are reduced by mercuric chloride ($HgCl_2$) and methylmercury (CH_3HgCl). *Neurotoxicology* **17:**85–92.

Manalis RS and Cooper GP (1975) Evoked transmitter release increased by inorganic mercury at frog neuromuscular junction. *Nature (Lond)* **257:**690–691.

Marty MS and Atchison WD (1997) Pathways mediating Ca^{2+} entry in rat cerebellar granule cells following *in vitro* exposure to methyl mercury. *Toxicol Appl Pharmacol* **147:**319–330.

McEnery MW, Vance CL, Begg CM, Lee WL, Choi Y, and Dubel SJ (1998) Differential expression and association of calcium channel subunits in development and disease. *J Bioenerg Biomembr* **30:**409–418.

Meir A and Dolphin AC (2002) Subunit interactions and channelopathies in Ca_v channels. *Modulator (Alamone Labs, Israel)* **16:**4–13.

Pan JQ and Lipscombe D (2000) Alternative splicing in the cytoplasmic II-III loop of the N-type Ca^{2+} channel α_{1B} subunit: functional differences are β subunit-specific. *J Neurosci* **20:**4769–4775.

Peng S-Q, Hajela RK, and Atchison WD (2002) Effects of methylmercury on human neuronal L-type calcium channels transiently expressed in human embryonic kidney cells (HEK293). *J Pharmacol Exp Ther* **302:**424–432.

Perez-Garcia MT, Kamp TJ, and Marban E (1995) Functional properties of cardiac L-type calcium channels transiently expressed in HEK293 cells. Roles of α_1 and β subunits. *J Gen Physiol* **105:**289–305.

Quefurth HW, Haughey NJ, Greenway SC, Yacono PW, Golan DE, and Geiger JD (1998) Expression of ryanodine receptors in human embryonic kidney (HEK293) cells. *Biochem J* **334:**79–86.

Randall A and Tsien RW (1995) Pharmacological dissection of multiple types of Ca^{2+} channel current in rat cerebellar granule neurons. *J Neurosci* **15:**2995–3012.

Rossi AD, Larsson O, Manzo L, Orrenius S, Vahter M, Berggren PO, and Nicotera P (1993) Modifications of Ca^{2+} signaling by inorganic mercury in PC12 cells. *FASEB J* **7:**1507–1514.

Sakamoto M, Ikegami N, and Nakano A (1996) Protective effects of Ca^{2+} channel blockers against methylmercury toxicity. *Pharmacol Toxicol* **78:**193–199.

Schirrmacher K, Wiemann M, Bingmann D, and Büsselberg D (1998) Effects of lead, mercury and methylmercury on gap junctions and $[Ca^{2+}]_i$ in bone cells. *Calcif Tissue Int* **63:**134–139.

Shafer TJ (1998) Effects of Cd^{2+}, $Pb^{2+}$and CH_3Hg^+ on high voltage-activated calcium currents in pheochromocytoma (PC12) cells: potency, reversibility, interactions with extracellular Ca^{2+} and mechanisms of block. *Toxicol Lett* **99:**207–221.

Shafer TJ and Atchison WD (1991) Methylmercury blocks N- and L-type Ca^{2+} channels in nerve growth factor differentiated pheochromocytoma cells. *J Pharmacol Exp Ther* **258:**697–702.

Sirois JE and Atchison WD (1996) Effects of mercurials on ligand- and voltage-gated ion channels: a review. *Neurotoxicology* **17:**63–84.

Sirois JE and Atchison WD (2000) Methylmercury affects multiple subtypes of calcium channels in rat cerebellar granule cells. *Toxicol Appl Pharmacol* **167:**1–11.

Stotz SC, Spaetgens RL, and Zamponi GW (2000) Block of voltage-dependent calcium channels by the green mamba toxin calcicludine. *J Membr Biol* **174:**157–165.

Sutton KG, Siok C, Stea A, Zamponi G, Heck SD, Volkmann RA, Ahlijanian MK, and Snutch TP (1998) Inhibition of neuronal calcium channels by a novel peptide spider toxin, DW13.3. *Mol Pharmacol* **54:**407–418.

Szucs A, Angiello C, Salanki J, and Carpenter DO (1997) Effects of inorganic and methylmercury on the ionic currents of cultured rat hippocampal neurons. *Cell Mol Neurobiol* **17:**273–288.

Tsien RW, Lipscombe D, Madison D, Bley K, and Fox A (1995) Reflections on calcium channel diversity, 1988–1994. *Trends Neurosci* **18:**52–54.

Weisenberg F, Bickmeyer U, and Wiegand H (1995) Effects of inorganic mercury on calcium channel currents and catecholamine release from bovine chromaffin cells. *Arch Toxicol* **69:**191–196.

Williams ME, Brust PF, Feldman DH, Patthi S, Simerson S, Maroufi A, McCue AF, Velicelebi G, Ellis SB, and Harpold MM (1992b) Structure and functional expression of an ω-conotoxin sensitive human N-type calcium channel. *Science (Wash DC)* **257:**389–395.

Williams ME, Feldman DH, McCue AF, Brenner R, Velicelebi G, Ellis SB, and Harpold MM (1992a) Structure and functional expression of α_1, α_2 and β subunits of a novel human neuronal calcium channel subtype. *Neuron* **8:**71–84.

Williams ME, Marubio LM, Deal CR, Hans M, Brust PF, Philipson LH, Miller RJ, Harpold MM, and Ellis SB (1994) Structure and functional characterization of neuronal α_{1E} calcium channel subtypes. *J Biol Chem* **269:**22347–22357.

Yuan Y and Atchison WD (1994) Comparative effects of divalent mercury, methylmercury and phenylmercury on membrane excitability and synaptic transmission of CA1 neurons in hippocampal slices of the rat. *Neurotoxicology* **15:**403–412.

Address correspondence to: Dr. Bill Atchison, Department of Pharmacology and Toxicology, Michigan State University, B-331 Life Sciences Bldg., East Lansing, MI 48824-1317. E-mail: atchiso1@msu.edu